Identification and functional analysis of *Penicillium digitatum* genes putatively involved in virulence towards citrus fruit

Mario López-Pérez[†], Ana-Rosa Ballester, Luis González-Candelas[*]

Instituto de Agroquímica y Tecnología de Alimentos (IATA-CSIC). Calle Catedrático Agustín Escardino 7, Paterna, 46980-Valencia Spain

[†] Present address: División de Microbiología. Universidad Miguel Hernández. Apartado 18, 03550-San Juan de Alicante

*Corresponding author:

Instituto de Agroquímica y Tecnología de Alimentos (IATA-CSIC). Calle Catedrático Agustín Escardino 7, Paterna, 46980-Valencia, Spain. Phone: +34 963900022. Fax: +34 963636301. E-mail: lgonzalez@iata.csic.es

Running title: Identification of *P. digitatum* virulence factors

Keywords: fruit-pathogen interaction, gene knockout, cell wall degrading enzymes, proteases, phytopathogenic fungi, gene expression

GenBank accession numbers: JZ350630 to JZ351000, KF466484 and KF466485.

Word count: 7030

SUMMARY

The fungus *Penicillium digitatum*, the causal agent of the green mould rot, is the most destructive postharvest pathogen of citrus fruit in Mediterranean regions. In order to identify *P. digitatum* genes up-regulated during the infection of oranges that may constitute putative virulence factors, we have followed a PCR-based suppression subtractive hybridization and cDNA macroarray hybridization approach. The origin of ESTs was determined by comparison against the available genome sequences of both organisms. Genes coding for fungal proteases and plant cell wall degrading enzymes represent the largest categories in the subtracted cDNA library. Northern blot analysis of a selection of *P. digitatum* genes, including those coding for proteases, cell wall related enzymes, redox homoeostasis and detoxification processes, confirmed their up-regulation at varying time points during the infection process. *Agrobacterium tumefaciens*-mediated transformation was used to generate knockout mutants for two genes encoding a pectin lyase (Pnl1) and a naphthalene dioxygenase (Ndo1). Two independent *P. digitatum* Δ*ndo1* mutants were as virulent as the wild type. However, the two Δ*pnl1* mutants analysed were less virulent than the parental strain or an ectopic transformant. Together, these results provide a significant advance in our understanding on the putative determinants of the virulence mechanisms of *P. digitatum*.

INTRODUCTION

Citrus are one of the world's major fruit crops. The filamentous fungus *Penicillium digitatum*, the causal agent of citrus green mould, is the main postharvest pathogen of citrus fruit. This ascomycete is a necrotroph that penetrates the fruit through wounds originated during harvesting and postharvest handling. Interestingly, *P. digitatum* shows a very narrow host range, as it does not infect any other fresh fruit or vegetable crop under natural conditions. The use of synthetic fungicides has been the standard procedure in many citrus-producing areas since the early 1970s to control this pathogen (Harding, 1972; Wild *et al.*, 1975). However, these chemical treatments have several disadvantages such as the persistence of the residues on the treated fruits, increased selective pressure for the appearance of pathogen resistant strains as well as health and environmental problems (Bus, 1992; Eckert, 1990). Thus, there is a need to study new alternatives of disease control that can replace the use of actual fungicides (Palou *et al*., 2008). Knowledge of the fruit's defence responses and pathogen's virulence are two fields that have begun to be explored in recent years. Most of the studies have been focused on the fruit, either analysing the response against pathogens (González-Candelas *et al.*, 2010) or the mechanisms underlying induced resistance (Ballester *et al.*, 2011). On the pathogen side, most of the work has dealt with fungicide resistance, although few studies addressing the functional analysis of specific genes have been published (Zhang *et al.*, 2013a, 2013b, 2013c). However, no systematic analysis of the *P. digitatum*'s virulence mechanism has been conducted so far, although the recently published genome of three *P. digitatum* strains can help us to identify genes involved in the virulence and specificity of this pathogen (Marcet-Houben *et al.*, 2012; Sun *et al.*, 2013). In the present work we aim to close this gap by studying at the molecular level the mechanisms involved in the pathogenicity of *P. digitatum*. We have isolated and

characterized *P. digitatum* genes that are up-regulated during the infection process and have functionally characterized two of them by targeted gene disruption.

RESULTS

In order to identify *P. digitatum* genes up-regulated during the infection of citrus fruit a subtractive cDNA library was constructed using RNA from *P. digitatum*-infected peel tissue collected at 3 dpi, when tissue maceration was first observed, as 'tester'. The 'driver' consisted of a mixture of RNAs obtained from *in vitro* grown fungus and non-infected fruit tissue. To estimate the relative amounts of fungus and fruit RNA in the infected tissue at 3 dpi, we compared the RNA from this tissue with different mixtures of fruit and *P. digitatum* RNAs. Quantification of the band corresponding to the fungal mitochondrial large-subunit rRNA allowed to estimate a 9:1 ratio of fungal to fruit RNA in the infected orange tissue at 3 dpi (Fig. S1, see Supporting Information), and this ratio was used to prepare the 'driver' RNA. The efficiency of the subtraction was analysed using two *P. digitatum* reference genes previously isolated in our group (González-Candelas *et al*., 2010) that show constitutive expression (Fig. 2). One codes for histone 3 (EKV08578) and the other for an actin like protein (EKV18284). Then, subtracted cDNA fragments were cloned into the plasmid pCRII, originating a subtractive cDNA library, named 'PDS'(NCBI Biosample 2141828).

Sequence analysis of the PDS library

The statistical analysis of the hybridization signals indicated that 867 clones (60.2 % of the total) showed a significant differential expression during infection, with 741 clones (51.5 % of the total) being up-regulated, demonstrating that the 'PDS' library is enriched in *P. digitatum* genes that are induced during infection of citrus fruit. A total of

371 valid sequences (GenBank accession numbers JZ350630 to JZ351000) were obtained from the sequenced clones, which included those with a ≥ 2 fold-induction in I3 over V3 (135 clones) and 236 randomly selected clones. Three hundred and six sequences mapped exclusively to the genome of *P. digitatum* isolate Pd1 (Marcet-Houben *et al*., 2012) and 28 to the genome of *C. sinensis* cv. Valencia (Xu *et al*., 2013). There were 35 chimeric sequences, 34 of them only contained *P. digitatum* sequences and one was a mixture of sequences from both organisms. Finally, there were only two sequences that did not map to either organism. The 371 ESTs were clustered into 161 unigenes (Table S1), yielding a redundancy of 56.6 %, which indicates that the subtracted cDNA library is composed of a small subset of sequences. These 161 unigenes are formed by 59 contigs and 102 singletons (Table 1), which corresponded to 112 genes from *P. digitatum*, 15 from *C. sinensis* and two unassigned genes. The remaining 32 unigenes corresponded to the 35 chimeric ESTs that were no further analysed.

The unigenes containing at least 3 ESTs are shown in Table 2. These 26 genes account for 203 ESTs, representing 54.7% of the total ESTs. Three unigenes, coding for a reticuline oxidase (SSH-12), a pathogen-inducible alpha-dioxygenase (SSH-17) and a DNA-binding protein (SSH-20), belong to *C. sinensis* and the rest of unigenes belong to *P. digitatum*. One unigene matches the mithocondrial DNA (SSH-09) and the remaining 22 unigenes match predicted genes in *P. digitatum*. The most represented unigene (SSH-01) contains 53 ESTs and correspond to the *P. digitatum* Pd1 PDIP_82060 protein, an aspartic endopeptidase. Interestingly, among the most abundant unigenes there are other four genes coding for proteases/peptidases: an aspergillopepsin (SSH-04), a tripeptidyl peptidase (SSH-05), a carboxypeptidase (SSH-08) and a serin peptidase (SSH-26). These five protease-related genes account for 88 ESTs and

represent the largest category in the cDNA library. A sixth protease encoding gene (PDS09C03, alkaline serine protease) is present in a chimeric clone.

The second most abundant group of unigenes (35 ESTs) correspond to different plant cell wall degrading enzymes (CWDE): two pectin lyases (SSH-15 and SSH-24), a polygalacturonase (PG; SSH-02) and an endoglucanase (SSH-03). Three of the 26 *P. digitatum* unigenes code for hypothetical proteins (SSH-07, SSH-13and SSH-21) of unknown function.

The remaining 103 unigenes (Table S1) include 133 ESTs. The main group, represented by 14 unigenes, includes several *P. digitatum* ribosomal proteins. Among these less abundant unigenes we also found several *P. digitatum* genes presumably related to pathogenesis, such as a glucanase (PDS09D07) and a pectinesterase (SSH-28). Another group includes different types of transporters: three oligopeptide transporters (SSH-41, PDS08H01 and PDS09C10) and three transporters involved in detoxification; two major facilitator superfamily (MFS) transporters (PDS09B02 and PDS-0024) and an ATP-binding cassette (ABC-type) transporter (SSH-55). Several unigenes are involved in redox metabolism, such as those coding for a thioredoxin (PDS09H05), a superoxide dismutase (PDS02D05), a peroxiredoxin (PDS-0017), a glutatione S-transferase (SSH-56), a NADPH:ubiquinone oxidoreductase (SSH-35) or several dehydrogenases. Other pathways or processes represented by more than one unigene are glycolysis and ubiquitination.

The results of the macroarray hybridization revealed that the unigenes with a larger representation in the PDS library also showed a high induction level in infected orange fruits (I3) over *in vitro* growth conditions (V3) (Table 3). Thus, the unigenes encoding the proteases aspergillopepsine (SSH-04), aspartic endopeptidase (SSH-01) and tripeptydil peptidase (SSH-05) are amongst the most highly up-regulated genes. The

genes encoding PG1 (SSH-02) and two pectin lyases (PSSH-24 and SSH-15) are also highly up-regulated. However, the unigene with the highest induction value (SSH-38) codes for an extracellular protein that contains a thaumatin domain (PDIP_76190), which is represented by only two ESTs. Another unigene that is highly induced during infection of citrus fruit and contains 10 ESTs is SSH-06, which codes for a concanamycin induced protein C (CipC, PDIP_45260).

Functional annotation

Ninety four out of the 112 *P. digitatum* unigenes had at least one associated GO term. The most abundant biological processes were related to translation and ribosome biogenesis (Fig. 1A). Processes related to nucleic acids, carbohydrates, carboxylic acids, phosphorylation and cation transport were also abundant. A high abundance of functions related to pathogenesis was observed (Fig. 1B), such as two hydrolases activities, peptidase activity and serine peptidase activity, although the most abundant category was metal ion binding. Other abundant functions involved the membrane, different oxidoreductases and activities related to nucleic acids.

Analysis of gene expression

Seventeen genes were selected for a more detailed analysis of their expression patterns based upon the macroarray hybridization results, their abundance or their possible involvement in pathogenicity. They were grouped into four major categories: proteolysis, plant cell wall degradation, fungicide resistance / detoxification and redox metabolism. We included a previously identified PG encoding gene (*pg2*, C34110E09) (Marques *et al.*, 2009) as well as a glyceraldehyde phosphate dehydrogenase (*gpdh*)

encoding gene, which in many filamentous fungi has been considered as a constitutively expressed gene.

All genes, except *cyp51B*, showed a higher expression during infection of citrus fruits than under *in vitro* growth conditions (Fig. 2). Even the *gpdh* gene showed a higher expression level in infected fruits. Most of the genes showed a maximal expression at 3 dpi, although the three pectinase encoding genes peaked at 1 (*pg1*) or 2 dpi (*pg2* and *pnl1*). The expression of the proteases, pectinases, naphthalene dioxygenase and the ABC transporter decreased at 4 and 7 dpi during infection of citrus fruit, whereas the other genes kept a relatively high expression level.

The patterns of expression observed during *in vitro* growth were different from those observed during the infection of oranges. Some genes were not expressed at all (SSH-08, carboxypeptidase) or showed a temporary expression at 0-1 dpi, as is the case for most of the proteases, the endoglucanase (SSH-03), *pg1* and the ABC transporter (SSH-55). The naphthalene dioxygenase and the PMR4 encoding genes showed a very weak expression and the remaining genes were expressed at all five time points. Interestingly, *pg2* was the only gene with maximum gene expression level at 4 dpi during *in vitro* growth.

Cloning and characterization of the *P. digitatum* genes *ndo1* and *pln1*

Protease encoding genes were the most abundant in the subtracted cDNA library. However, their high redundancy is detrimental for functional analysis, because the lack of a gene in a knockout mutant can be compensated by another gene encoding a protein with similar properties. Thus, on the bases of their annotations and expression patterns we selected for further functional characterization two genes belonging to different categories. Within the group of genes related to redox metabolism we selected the gene

ndo1 (SSH-22), which codes for the alpha subunit of a napththalene 1,2-dioxygenase. The expression of this gene was much higher during infection of citrus fruits than during *in vitro* growth (Fig. 2). Within the plant cell wall degradation category we selected the gene *pnl1*, which codes for pectin lyase 1, as the encoded protein could be responsible for the maceration of the host tissue without the intervention of additional proteins. Two fosmids containing both genes were isolated from the genomic library following a PCR-based screening. A DNA fragment of 4971 bp was sequenced in the fosmid containing the *ndo1* gene, including 1948 bp in the promoter region and 1728 bp in the 3' downstream region (GenBank Acc. No. KF466485). The *ndo1* gene is 1296 bp in length and is interrupted by one intron of 54 bp. The predicted Ndo1 protein is 413 aa in length and is identical to the *P. digitatum* PHI26 EKV19050 protein (PDIG_04590). However, it is 36 aa larger than the *P. digitatum* Pd1 EKV21060 protein (PDIP_10140). This difference is due to the presence of a 'TC' insertion within the first exon of the gene with respect to the previously determined genome sequence of *P. digitatum* Pd1 obtained by pyrosequencing. The same sequence of *ndo1* is present in the strain Pd01-ZJU. The predicted Ndo1 protein (EC:1.13.11.0) is an intracellular protein that contains the canonical N-terminal (cd03469) and C-terminal (cd00680) domains of Rieske non-heme iron aromatic ring-hydroxylating oxygenase alpha subunit family of proteins. These proteins participate in the oxidative degradation of aromatic compounds catalysing the addition of hydroxyl groups to the aromatic ring employing iron as a cofactor. The protein Ndo1 shares sequence identity above 70 % along the whole protein with other putative fungal naphthalene dioxygenases.

The nucleotide sequence of a 5302 bp fragment containing the *pnl1* gene was determined (GenBank Acc. No. KF466484). The coding sequence of *pnl1* is 1366 bp in length and is interrupted by four introns (56, 60, 72 and 56 bp). The flanking promoter

(2080 bp) and terminator (1856 bp) regions do not contain any predicted gene. There is a complete agreement in the nucleotide sequence with those derived from the genomes of *P. digitatum* Pd1, PHI26 and Pd01-ZJU previously determined by next generation sequencing (Marcet-Houben *et al*., 2012; Sun *et al*., 2013). However, the protein Pnl1 (PDIP_08080) contains 6 aa that are absent in the protein deduced from the Pd01_ZJU strain. This difference is due to the size of this first intron, which is 18 bp shorter in Pd1. We have established the correct intron position by sequencing a full-length cDNA obtained from clone C34104G01 (Marques *et al*., 2009). Thus, Pnl1 is a pectin lyase (EC 4.2.2.10) of 373 aa that contains a secretion signal peptide of 19 aa. It belongs to the polysaccharide lyase family 1 (PL1) of CAZYmes (Carbohydrate Active Enzymes) and is closely related to other fungal pectin/pectate lyases, with identity values above 70% all over the sequence. The most similar non *Penicillium* protein is the pectin lyase D of *Aspergillus niger* (P22864).

Targeted disruption of the *P. digitatum ndo1* and *pnl1* genes

The promoter and terminator regions of both genes were introduced into the plasmid pRF-HU2 to obtain the plasmids pRFDNDO1 and pRFDPNL1 (Fig. 3A and Fig. 4A, respectively). After *A. tumefaciens*-mediated transformation of *P. digitatum* Pd1, we screened by PCR 50 and 56 transformants of *ndo1* and *pnl1* genes, respectively, to confirm the presence of the hygromycin gene using the oligonucleotides HMBF1 and HMBR1 (Table 4). The expected 801 bp PCR fragment was detected in all transformants and was absent in the untransformed Pd1 strain (Fig. 3C and Fig. 4C). Deletion of the target genes *ndo1* and *pnl1* was detected by using primers RP6S+RP5A and PL6S+PL5A, respectively, that are present in both the wild type untransformed Pd1 strain and in the T-DNA, as shown schematically in Fig. 3B and Fig. 4B. In most of the

transformants there were two amplicons of different sizes, one corresponding to the wild type locus and the other to the T-DNA construction. However, in Δ*ndo1* and Δ*pnl1* transformants there was only one amplicon corresponding to the T-DNA, because the target gene was no longer present. Thus, 13 out of the 50 and 6 out of 56 analysed *ndo1* and *pnl1* transformants were knockout mutants. Monosporic isolates were obtained from these transformants and were further validated by PCR using primers located within the coding region (RP7S+RP8A for *ndo1*, and PLS1+PLA1 for *pnl1*), which is not present in the T-DNA. As expected, these primers amplify the wild type and the ectopic transformants but failed to amplify in the knockout Δ*ndo1* and Δ*pnl1* transformants (Fig. 3C and Fig. 4C). Further confirmation of the deletion of the target gene was obtained using primers that flank either the 5' or the 3' end of the construction in combination with primers within the hygromycin resistance marker (RP8S+HPHTER2 and RP7A+HPHPR04 for *ndo1*, and PL8S+HPHTER2 and PL7A+HPHPR04 for *pnl1*), as only homologous recombinants (deletants) would amplify with these two primer pairs.

For each gene, four knockout and two ectopic transformants were selected for determining the number of T-DNA copies integrated in the genome by qPCR using the wild type Pd1 strain as a control and the beta-tubulin encoding gene as a reference (Table S2; primer pairs RPPrSA+RPPrS for *ndo1*, PLPrA+PLPrS for *pnl1*, and betatubPDIG1+betatuPDIG2 for beta-tubulin encoding gene). The four Δ*ndo1*mutants contained a single T-DNA integration. However two of the Δ*pnl1* mutants contained an extra T-DNA copy integrated elsewhere in the genome. For each gene, we selected two deletants containing a single T-DNA integration and an ectopic transformant as a control for further analysis.

Morphology and sporulation of the two knockout and the ectopic mutants were similar to those of the wild type Pd1 in both *ndo1* and *pnl1* transformants (Fig. 5A and Fig. 5C). In order to evaluate the role of these two genes in virulence, pathogenicity tests were conducted in orange fruits with the wild type *P. digitatum* Pd1, one ectopic and two knockout mutants (see Experimental procedures). Three independent infection assays were conducted. Disease severity was determined as the decayed area (cm^2) of the macerated area at 5 dpi. The results show that the *P. digitatum* Δndo1-10 and Δndo1-19 null mutants were as virulent as the wild type Pd1 strain and the ectopic ndo1-10 transformant in all the three experiments (Fig. 5B). However, in the three independent infection assays the Δpnl1-6 Δpnl1-7 and mutants were less virulent than the parental strain and the ectopic pnl1-9 transformant (Fig. 5D). Taking into account the three experiments, the average reduction in disease severity of the Δ*pnl1* mutants was 35% in comparison with the wild type Pd1 strain (Fig. 5D).

DISCUSSION

P. digitatum is the most important postharvest pathogen of citrus fruit. In recent years our knowledge on different aspects of its biology has increased enormously. However, no study has been conducted yet to identify *P. digitatum* genes involved in pathogenicity. For that purpose we constructed a SSH cDNA library enriched in *P. digitatum* genes that are up-regulated during the infection of citrus fruits in comparison to *in vitro* growth. cDNA macroarray hybridization showed that half of the clones were up-regulated during the infection process. A total of 371 sequences obtained from selected clones were grouped into 161 unigenes, most of them were of fungal origin. The high redundancy level of 56.6% suggests that the subtraction process was successful and the library is enriched in a relatively small group of genes.

More than 30% of the sequences obtained from the cDNA library belonged to protease/peptidase encoding genes and CWDE. Five genes corresponded to proteases (SSH-01, SSH-04, SSH-05, SSH-08 and SSH-26) and four code for CWDE (SSH-02, SSH-03, SSH-15 and SSH-24). Gene ontology annotation of the fungal unigenes (Fig. 1A) indicated that the most represented biological processes are related to amino acid and protein metabolism, biosynthesis of molecules and energy production by the cell, suggesting that all processes related to primary metabolism are overexpressed. Proteolysis was the only category related to the pathogenesis. This result agrees with the abundance of proteases obtained in the library and highlights the importance of this set of proteins in the pathogenicity of *P. digitatum*, a fact that has not been previously described in any fruit-fungus interaction. Regarding the molecular function classification (Fig. 1B), categories related to the requirements of a pathogenic lifestyle were highly represented. These categories comprise not only peptidase activity, but also hydrolase activities. However, metal ion, purine and ribonucleotide binding, together with the transmembrane transporter activity, are the most abundant molecular function categories present in the cDNA library. The abundance of proteins associated with metal ions highlights the relevance of metal homeostasis during the pathogenic growth of *P. digitatum*, as it has been already shown in other phytopathogenic fungi (Eichhorn *et al.*, 2006; Haas *et al.*, 2008). Gene expression analysis of 17 selected genes related to proteolysis, CWDE, detoxification and redox metabolism further showed that all of them, except *cyp51B*, showed a higher expression level during the infection of citrus fruits than under *in vitro* growth conditions (Fig. 2), thus validating the subtracted cDNA library.

Proteases constitute the largest group of *P. digitatum* genes up-regulated during infection of citrus fruits. Almost 24% of the ESTs present in the cDNA library belong to genes encoding proteases/peptidases, including an aspartic endopeptidase, a tripeptidyl peptidase, an aspergillopepsine, a serine peptidase, and a carboxypeptidase 5 (Table 2). All of them were up-regulated during infection of citrus fruits, showing a maximum of mRNA accumulation at 3 dpi (Fig. 2). Similarly, proteases were found among the most highly induced genes in *B. cinerea* during infection of sunflower cotyledons (Amselem *et al*, 2011). Proteases might contribute to pathogenicity in different ways, such as degrading plant cell wall components, providing a nitrogen supply for the organism when inorganic nitrogen in the environment has been depleted or even inactivating defence proteins (Naumann and Price, 2012). Although proteases are produced during infection by phytopathogenic fungi (Poussereau *et al.*, 2001; ten Have *et al.*, 2004) their possible role(s) in pathogenesis has not been unequivocally established. Targeted gene disruption of the *Magnaporthe grisea SPM1* gene, which codes for a vacuolar serine protease, resulted in greatly attenuated virulence (Donofrio *et al.*, 2006). However, single and double *B. cinerea* mutants lacking five different aspartic proteinase encoding genes were as virulent as the parental strain (ten Have *et al.*, 2010). Recently, it has been shown that class IV chitinases from different plants are truncated by proteases secreted by specialized fungal pathogens of each plant, suggesting that this may be a general mechanism of plant–fungal pathogenicity (Naumann *et al*., 2012)

The success of the infection depends on the pathogen's ability to penetrate and colonize the host tissues as well as its ability to degrade the cell wall polymers to obtain the nutrients required for its development. Therefore, enzymatic degradation of the extracellular polymers is traditionally considered an important aspect in fungal phytopathogens (see di Pietro *et al.*, 2009 for a review). Many CWDE are included in

the superfamily CAZymes. A recent comparative genomics analysis has shown that plant pathogenic fungi contain more CAZyme genes than saprophytic fungi and that biotrophic fungi have fewer CAZymes in comparison with necroptrophic and hemibiotrophic fungi (Zhao *et al.*, 2013). In the present work the importance of CWDE in the virulence of *P. digitatum* was highlighted because they constitute the second most abundant group of genes in the cDNA library with 39 ESTs. They belong to 7 genes encoding two pectin lyases (*pnl1* and *pnl2*), one polygalacturonase (*pg1*), one pectin methyl esterase and three glucanases (Table S1). Differential expression during pathogenesis of four of these genes, as well as that of a previously isolated PG encoding gene (*pg2*), was corroborated by Northern blot analysis (Fig. 2). The two PG encoding genes showed a high up-regulation during infection but they differ during axenic growth. It is noteworthy the high expression level of *pg1* at just 1 dpi, when the rest of the analysed genes were barely expressed. The expression of *pg2* and *pnl1* peaked at 2 dpi during infection of citrus fruits, showing a pattern of expression similar to that described by (Zhang *et al*., 2013b) in another *P. digitatum* strain. The two glucanase genes, SSH-03 and PDS09D07, also showed some differences in their expression patterns, mainly during *in vitro* growth. The different patterns of expression of the genes coding these CWDE suggest the presence of different transcriptional regulatory mechanisms. In this context it is interesting to note that many of these CWDE genes are expressed during *in vitro* growth in a medium rich in glucose, a common carbon catabolite repressor molecule (Aro *et al.*, 2005). It has been recently shown that the expression of *pg2* and *pnl1* during infection of citrus fruits is under the control of the pH responsive transcription factor PacC (Zhang *et al*., 2013a), whereas other *P. digitatum* CWDE encoding genes are under the positive control of the protein kinase SNF1 (Zhang *et al*., 2013b).

The role of specific CWDE in pathogenicity has been studied in phytopathogenic fungi, including postharvest pathogens such as *Alternaria alternata* (Eshel et al., 2002), *Colletotrichum gloesporoides* (Yakoby *et al*., 2001) or *Penicillium expansum* (Sánchez-Torres and González-Candelas, 2003), and their contribution to virulence has been demonstrated (Isshiki *et al*., 2001; Kars *et al*., 2005; ten Have *et al*., 1998). In *P. digitatum*, pectinases have been shown to play an important role in colonization and maceration of citrus fruit. A pectin lyase purified from culture supernatants and a polygalacturonase isolated from infected fruit tissue were able to macerate the peel of citrus fruits (Barmore and Brown, 1979; Bush and Codner, 1968). The recent availability of gene transformation tools for *P. digitatum* has allowed dissecting the role of individual genes in pathogenicity. The contribution of PG2 to virulence has been shown by analysing a *P. digitatum* Δ*pg2* deletion mutant, which showed lower virulence towards citrus fruits than the parental strain (Zhang *et al*., 2013b). A further evidence on the involvement of CWDE in *P. digitatum*'s virulence has been obtained from a *P. digitatum* Δ*snf1* mutant, which was impaired in the expression of several CWDE encoding genes and showed lower virulence than the parental strain (Zhang *et al*., 2013b).

Among the genes encoding CWDE, the *pnl1* gene showed the highest induction, reaching a maximum expression at 2 dpi (Fig. 2). Based on this pattern of expression and the fact that the encoded protein could macerate the citrus peel tissue, we analysed its role in pathogenicity by obtaining gene replacement mutants. Three independent infection assays were performed with two independent Δ*pnl1* mutants. The results (Fig. 5D) showed that disruption of *pnl1* resulted in 35% lower virulence as compared to either the parental strain or an ectopic transformant, demonstrating that Pnl1 contributes to full virulence of *P. digitatum* towards citrus fruit. The reduction of virulence

observed in Δ*pnl1* mutants is similar to that observed in the Δ*pg2* mutant (Zhang *et al*., 2013a), further supporting the role in pathogenicity of specific CWDE.

Another important group of genes isolated in the subtracted library is related to fungicide resistance or detoxification, including genes coding for ABC and MFS transporters, a sterol 14α-demethylase Cyp51B, and a CipC protein. Cyp51B is a sterol 14α-demethylase essential for the ergosterol biosynthesis, the predominant sterol in fungal membranes, the target enzyme of azole fungicides against various phytopathogenic fungi such as *M. grisea* (Yan *et al.*, 2011) or *P. digitatum* (Hamamoto *et al.*, 2000). Northern analysis showed high expression in both, infection and growth in liquid culture medium, suggesting that this gene is not essential during the infection process.

ABC transporters involved in imazalil resistance have been analysed in *P. digitatum* (Sun *et al*., 2013), but their role in virulence remains to be elucidated. PMR4 was isolated in the subtracted library (SSH-55/PDIP_53810), and its differential expression during the infection suggests that this transporter is not only important to fungicides resistant but also in the virulence of *P. digitatum*. Together with ABC transporters, MFS transporters are the most important efflux pumps involved in fungal protection against fungicides with remarkably broad substrate specificity, although they are also capable of transporting specific compounds (De Waard *et al.*, 2006, Stergiopoulos *et al.*, 2002). A membrane efflux transporter *P. digitatum MFS* gene (*PdMfs1*, AM412556.1, PDIP_62090) has already been cloned and showed to partially contribute to imazalil resistance, and also plays a role on the virulence of the pathogen (Wang *et al.*, 2012). We isolated another MFS transporter encoding gene (PDS09B02) from the 'PDS' library that showed up-regulation during the fruit-fungus interaction (Fig. 2).

Production of reactive oxygen species (ROS) is one the first responses deployed by plants against pathogens (Mehdy, 1994). It has been shown that *P. digitatum* is able to suppress the production of hydrogen peroxide in the host tissue during infection of citrus fruit (Macarisin *et al.*, 2007). In the subtracted library we identified a group of genes involved in oxidative stress metabolism (Table S1), including enzymes that produce hydrogen peroxide. The expression of three ROS-related genes was analysed by Northern blot hybridization and they were induced during the infection process (Fig. 2), suggesting that these genes may have an important role in the virulence of the fungus preventing the ROS-dependent defence of the fruit. The involvement in pathogenicity of SOD and NADPH:ubiquinone oxidoreductase has been demonstrated in other necrotrophic fungi (Rolke *et al.*, 2004; Seong *et al.*, 2005; Veluchamy *et al.*, 2012; Xu and Chen, 2012), whilst other fungal ROS-related genes, such as catalase and glutathione-S-transferase, seem to be dispensable for full virulence (Prins *et al.*, 2000; Schouten *et al.*, 2002).

Based on its expression prolife, we focused on the gene *ndo1*, which was up-regulated during infection but was barely expressed in axenic culture (Fig. 2), for further functional analysis. Although the exact function of the Ndo1 protein is not known, according to its structure it is probably involved in the metabolism of aromatic compounds, either to be used as nutrients or in their detoxification. Two independent Δ*ndo1* mutants containing a single T-DNA integration were characterized. They showed no differences with respect to the parental strain or an ectopic transformant in growth rate and sporulation in PDA medium. In three independent infection experiments these two deletant strains showed the same virulence as the parental strain or the ectopic transformant (Fig. 5D), indicating that this gene is dispensable for pathogenesis in *P. digitatum*.

In conclusion, we have identified a number of *P. digitatum* genes that are up-regulated during the infection of citrus fruit. Four major groups of genes were found: proteases, CWDE, fungicide resistance/detoxification and redox metabolism. Further functional characterization has shown that *pnl1*, which codes for a pectin lyase, contributes to full virulence of *P. digitatum*, whereas *ndo1*, which codes for a naphthalene dioxygenase, is dispensable. This work, together with the availability of the genome sequence provides the basis for the identification of putative virulence factors of this important postharvest pathogen of citrus fruit.

EXPERIMENTAL PROCEDURES

Fruit and fungal materials

'Navelina' orange fruits (*Citrus sinensis* L. Osbeck) were harvested in a commercial orchard in Lliria (Valencia, Spain) and processed the same day. Oranges were surface-sterilized with a 5 % commercial bleach solution for 5 min, washed with tap water and dried at room temperature until next day. Conidia from *Penicillium digitatum* Sacc. isolate Pd1 (CECT20795;(Marcet-Houben *et al.*, 2012) were collected from a seven-day-old culture grown on potato dextrose agar (Difco) at 24 ºC by scraping them with a sterile spatula and transferred to sterile distilled water. Conidia concentration was determined with a haemocytometer.

For RNA extraction, mycelium of *P. digitatum* was obtained by inoculating 10^5 conidia ml^{-1} into 500 ml of potato dextrose broth (PDB, Difco) followed by incubation at 24 ºC and 200 rpm for up to 96 h. For DNA extraction the fungus was incubated in PDB for 48 h at 24 ºC and 200 rpm. Mycelium was filtrated through a nylon mesh, washed twice with sterile distilled water, dried between paper towels and frozen in liquid nitrogen before being stored at -80 ºC until RNA isolation.

Fruit infections

Fruits were inoculated at 12 points by making punctures with a nail (approximately 3 mm in depth) and adding 10 µL of a conidial suspension adjusted to 10^6 conidia mL^{-1} and incubated in plastic boxes at 90% relative humidity (RH) and 20 ºC for up to 7 d. Peel discs of 7 mm in diameter around the inoculation site were obtained with a cork borer. They were immediately frozen in liquid nitrogen, grounded to a fine powder with a coffee mill and stored at −80 ºC until RNA extraction.

Pathogenicity tests

Fruits were wounded at four places around the equatorial axis and inoculated with 10 µL of a conidial suspension adjusted to 10^4 conidia mL^{-1}. Then, they were kept at 20 ºC and 90 % RH. There were three replicates of five fruits each. The severity of the infection, measured as the decayed area (cm^2), was determined at 5 dpi. ANOVA was performed to test the different incidence among mutants. Means were separated using LSD test with $P < 0.05$ using Statgraphics Plus 5.1 (Manugistics Inc.).

Construction of a *P. digitatum* genomic DNA library

DNA was extracted from 1 g of frozen mycelium essentially as described by Moller *et al* (1992). Size-selected and end-repaired DNA was ligated into linearized fosmid pCC2FOS using the CopyControl HTP Fosmid Library Production kit (Epicentre Biotechnologies). Ligated DNA was packaged with the MaxPlax Lambda Packaging Extracts provided in the kit and transfected into *E. coli* EPI300 cells following the supplier's recommendations.

RNA extraction

RNA was isolated from 2 g of peel tissue discs or 1 g of frozen mycelium according to the protocol described by Ballester *et al*. (2006) with minor modifications. After phenol:chloroform extraction, RNA was precipitated from the aqueous phase by adding lithium chloride to a final concentration of 3 M and incubating at -20 ºC for at least twelve hours. Poly(A)$^+$ RNA was separated from total RNA using the Dynabeads® mRNA Purification^{TM} kit according to the manufacturer's protocol (Invitrogen).

Construction of a subtracted cDNA library

cDNA synthesis and the Supression Subtractive Hybridization (SSH) procedure (Diatchenko *et al.*, 1996) were carried out using the PCR-Select^{TM} cDNA Subtraction kit (Clontech) according to the protocol supplied by the manufacturer. We used a mixture of RNAs from non-infected fruits and *in vitro* grown fungus as a 'driver' and RNA from *P. digitatum*-infected fruit tissue at 3 days post-inoculation (dpi) as 'tester'. One microgram of poly(A)$^+$ RNA from the 'tester' and the 'driver' were used for cDNA synthesis. Subtracted cDNA fragments were ligated into the cloning vector pCRII (Invitrogen) and transformed into *Escherichia coli* DH5α competent cells by electroporation.

cDNA sequencing and EST analysis

Plasmids were sequenced with primer SP6 (Table 4) and the BigDye terminator kit v1.1 (Applied Biosystems). Raw sequences obtained were trimmed off vector and adaptor sequences with the program CLC Genomics Workbench (CLC Bio, Qiagen).

Sequencing processing and mapping of the ESTs to the *P. digitatum* isolate Pd1 (Marcet-Houben *et al*., 2012) and *Citrus sinensis* cv. Valencia (Xu *et al*., 2013) genomes were done with the same program. Gene ontology annotation of unigenes was conducted with the program Blast2GO (Conesa and Gotz, 2008).

Northern blot analysis

Northern blot analysis was conducted as described previously (Ballester *et al*., 2006). Primer FOR17 (Table 4) was used for labelling the probe corresponding to the *P. digitatum* 28S rDNA (GenBank acc. no. AJ969116) and primer N2R (Table 4) for the rest of the clones derived from the subtracted cDNA library.

Macroarray design, hybridization and data analysis

Replicated nylon membranes containing 1536 spots, corresponding to 1440 amplicons from randomly picked colonies and eight different positive and negative controls, spotted in replicate positions, were prepared in a macroarray spotting service (SCSIE, Universitat de València, Spain). Then, each macroarray was hybridized with ^{33}P-labeled cDNA probes derived from total RNA of either infected fruit tissue at 3 dpi (denoted as 'I3') or *P. digitatum* mycelium grown *in vitro* for 3 d in PDB (denoted as 'V3'). Three independent biological replicate hybridizations were conducted. First strand cDNA synthesis, macroarray hybridization and signal analysis were carried out as previously described (González-Candelas *et al*., 2010). Only signal values 1.3 times over the corresponding background and derived from at least two replicate hybridizations were taken as valid measurements. Statistical analysis was done with the ArrayStat software (Imaging Research) as described previously (González-Candelas *et al*., 2010).

Gene knockout plasmid constructions

Plasmids were constructed following the protocol described by Crespo-Sempere *et al.* (2011). The promoter and terminator regions of the *ndo1*gene were amplified from fosmid DNA with primers pairs RPO1+RPO2 and RPA3+RPA4, respectively (Table 4). The promoter and terminator regions of the *pnl1*gene were amplified with primers pairs PLO1+PLO2 and PLA3+PLA4, respectively (Table 4). Plasmids pRFDNDO1 and pRFDPNL1 (Fig. 3A and 4A, respectively) were obtained by cloning the amplified fragments into the plasmid vector pRF-HU2 (Frandsen *et al.*, 2008), which was previously digested with *PacI* and *Nt.BbvCI*, following the USER friendly cloning technique (New England Biolabs). An aliquot of each plasmid was used to transform *E. coli* XL1-blue chemical competent cells. Kanamycin resistant transformants were screened by PCR. Proper fusion was confirmed by DNA sequencing. Then, both plasmids were introduced into electrocompetent *A. tumefaciens* AGL-1 cells.

Agrobacterium tumefaciens*-mediated transformation of *Penicillium digitatum

A. tumefaciens AGL-1 cells carrying either plasmid pRFDNDO1 or pRFDPNL1 were used for *P. digitatum* transformation as described previously (Marcet-Houben *et al.*, 2012). Hygromcycin resistant colonies were transferred to PDA containing hygromycin (100 µg mL^{-1}) to isolate monosporic transformants. Conidia were inoculated into 500 µl of GPY liquid medium supplemented with hygromycin (100 µg mL^{-1}) and incubated for 2 d at 24 ºC and 200 rpm. Mycelium was collected and stored at -20 ºC until DNA extraction.

Molecular characterization of transformants

DNA extraction from fungal mycelium was done according to Cenis (1992) in 2 ml tubes containing five 2.7 mm steel beads and 300 µL of TNES (200 mM Tris-HCl, pH 8.5, 250 mM NaCl, 25 mM EDTA, 0.5 % SDS) with the aid of a Mini Beadbeater 8 Cell Disruptor (Biospec Products). Insertion of the T-DNA in the transformants was verified by PCR with the primers HMBF1+HMBR1 (Table 4), which target the hygromycin resistance gene. Deletion of the targeted gene was analysed with primers RP6S-RP5A and PL6S-PL5A (Table 4) for the *nod1* and *pnl1* genes, respectively. The absence of the targeted gene in the deletants was further verified using the primers RP7S+RP8A and PL1S+PL1A (Table 4) for the *nod1* and *pnl1* genes, respectively. Figures 3B and 4B show a scheme with the relative position of the primers used in the characterization of the transformants.

The number of T-DNA insertions integrated in each selected transformant was assessed by quantitative PCR (qPCR) analysis following the procedure described by Crespo-Sempere *et al.* (2013) using primers located in the promoter region of the *pnl1* (PLPrS+PLPrA) and *ndo1* (RPPrS+RPPrA) genes (Table 4). The *P. digitatum* gene encoding the beta-tubulin (GenBank Acc. No. GU124566) was used as a reference for normalization using primers betatubPDIG1 and betatubPDIG2 (Table 4). DNA from the wild type Pd1 strain was used as a control. PCR reactions and data analysis were done using a LightCycler 2.0 Real-Time PCR machine (Roche) and the LightCycler software, version 4.0, according to the manufacturer`s instructions.

ACKNOWLEDGEMENTS

The technical assistance of Ana Izquierdo (IATA-CSIC, Valencia, Spain) is gratefully acknowledged. LGC research is funded in part by the Spanish Ministry of Economy and Innovation (AGL-2008-04828-C03-02 and AGL2011-30519-C03-01) and the Generalitat Valenciana (PROMETEO/2010/010, PROMETEOII/2014/027 and ACOMP/2011/250). MLP was supported by a FPI scholarship (BES-2006-12983). ARB acknowledges the support of the JAE-Doc program from CSIC cofounded by FSE. Authors declare no conflict of interest.

TABLE AND FIGURE LEGENDS

Table 1. Summary of the subtracted cDNA library PDS.

Table 2. Identification of *P. digitatum* and *C. sinensis*-responsive genes isolated from the SSH library in infected orange fruits containing three or more ESTs.

Table 3. Genes with a 2-fold or higher induction level at 3 days post infection in orange fruits inoculated with *P. digitatum* with respect to *in vitro* growth conditions.

Table 4. Oligonucleotides used in the present work

Fig. 1. Gene ontology (GO) analysis of the 161 *P. digitatum* unigenes obtained in the 'PDS' subtracted cDNA library showing biological process category (level 5) (A) and molecular function category (level 5) (B). The analysis was carried out with Blast2GO.

Fig. 2. Northern blot analysis of clones selected from the 'PDS' library. Membranes were hybridized with probes corresponding to: aspartic endopeptidase (SSH-01), tripeptidyl peptidase (SSH-05), aspergillopepsin (SSH-04), serine peptidase (SSH-26), carboxypeptidase 5 (SSH-08), endoglucanase (SSH-03), polygalacturonase 1 (SSH-02), polygalacturonase 2 (C34110E09), glucanase (PDS09D07), pectin lyase 1 (SSH-15), thioredoxin (SSH-42), superoxide dismutase (PDS02D05), naphthalene 1,2-dioxygenase (SSH-22), ABC transporter, PMR4 (SSH-55), MFS transporter (PDS09B02), demethylase Cyp51B (SSH-42), CipC protein (SSH-06), glyceraldehyde 3-phosphate dehydrogenase (GPDH, SSH-10), histone H3 (C06004H02) and actin like protein (C06016B0). Normalization of hybridization signals was carried out with respect to the hybridization signal of the *P. digitatum* 28S rDNA. Values below the panels show the relative quantification of the corresponding hybridization signal referred to the value of the infected sample at 3 days (d) post-inoculation (dpi). The analysis was carried out at 1, 2, 3, 4 and 7 d after infection of orange fruits with *P. digitatum* (infection), and at 0, 1, 2, 3 and 4 d of *P. digitatum* incubation in potato dextrose broth medium (*in vitro*). Orange fruit RNA at 3 d after wound practice was used as a control.

Fig. 3. Analysis of *P. digitatum ndo1* transformants. (A) Map of plasmid pRFDNDO1. (B) Diagram of wild type locus and the *ndo1* replacement with the Hyg^R selectable marker from pRFDNDO1 by homologous recombination to generate the Δ*ndo1* mutant. Primers used in the construction of plasmid pRFDNDO1 and those used for analysis of transformants are shown. (C) PCR analysis of the wild type Pd1 strain, an ectopic (ndo1-12) and two knockout (Δndo1-10 and Δndo1-19) transformants.

Fig. 4. Analysis of *P. digitatum pnl1* transformants. (A) Map of plasmid pRFDPNL1. (B) Diagram of wild type locus and the *pnl1* replacement with the Hyg^R selectable marker from pRFDPNL1 by homologous recombination to generate the Δ*pnl1* mutant. Primers used in the construction of plasmid pRFDPNL1 and those used for analysis of transformants are shown. (C) PCR analysis of the wild type Pd1 strain, an ectopic (pnl1-9) and two knockout (Δpnl1-6 and Δpnl1-7) transformants.

Fig. 5. *In vitro* growth (A, C) and decayed area in cm^2 (B, D) of *ndo1* (A, B) and *pnl1* (C, D) mutants at 5 dpi. Wild type *P. digitatum* Pd1 (black bar), one ectopic mutant (dark grey bars) and two knockout mutants (white and light grey bars, indicated by 'Δ') were analyzed. Three independent experiments were performed. Bars indicated the decayed area in cm^2 plus the standard deviations calculated form three replicates of five fruit and four wounds per fruit. Different letters indicate significant differences among samples (LSD, $P < 0.05$).

REFERENCES

Amselem, J., Cuomo, C.A., van Kan, J.A.L., Viaud, M., Benito, E.P., Couloux, A., Coutinho, P.M., de Vries, R.P., Dyer, P.S., Fillinger, S., Fournier, E., Gout, L., Hahn, M., Kohn, L., Lapalu, N., Plummer, K.M., Pradier, J.-M., Quévillon, E., Sharon, A., Simon, A., ten Have, A., Tudzynski, B., Tudzynski, P., Wincker, P., Andrew, M., Anthouard, V., Beever, R.E., Beffa, R., Benoit, I., Bouzid, O., Brault, B., Chen, Z., Choquer, M., Collémare, J., Cotton, P., Danchin, E.G., Da Silva, C., Gautier, A., Giraud, C., Giraud, T., Gonzalez, C., Grossetete, S., Güldener, U., Henrissat, B.,

Howlett, B.J., Kodira, C., Kretschmer, M., Lappartient, A., Leroch, M., Levis, C., Mauceli, E., Neuvéglise, C., Oeser, B., Pearson, M., Poulain, J., Poussereau, N., Quesneville, H., Rascle, C., Schumacher, J., Ségurens, B., Sexton, A., Silva, E., Sirven, C., Soanes, D.M., Talbot, N.J., Templeton, M., Yandava, C., Yarden, O., Zeng, Q., Rollins, J.A., Lebrun, M.-H. and Dickman, M. (2011) Genomic analysis of the necrotrophic fungal pathogens *Sclerotinia sclerotiorum* and *Botrytis cinerea*. *PLoS Genet.* **7,** e1002230.

Aro, N., Pakula, T. and Penttila, M. (2005) Transcriptional regulation of plant cell wall degradation by filamentous fungi. *FEMS Microbiol. Rev.* **29,** 719-739.

Ballester, A.R., Lafuente, M.T., Forment, J., Gadea, J., De Vos, C.H.R., Bovy, A.G. and González-Candelas, L. (2011) Transcriptomic profiling of citrus fruit peel tissues reveals fundamental effects of phenylpropanoids and ethylene on induced resistance. *Mol. Plant Pathol.* **12,** 879-897.

Ballester, A.R., Lafuente, M.T. and González-Candelas, L. (2006) Spatial study of antioxidant enzymes, peroxidase and phenylalanine ammonia-lyase in the citrus fruit-*Penicillium digitatum* interaction. *Postharvest Biol. Technol.* **39,** 115-124.

Barmore, C.R. and Brown, G.E. (1979) Role of pectplytic enzymes and galacturonic acid in citrus fruit decay caused by *Penicillium digitatum*. *Phytopathology* **69,** 675-678.

Bus, V.G. (1992) ED50 levels of *Penicillium digitatum* and *P. italicum* with reduced sensitivity to thiabendazole, benomyl and imazalil. *Postharvest Biol. Technol.* **1,** 305-315.

Bush, D.A. and Codner, R.C. (1968) The nature of macerating factor of *Penicillium digitatum Phytochemistry* **7,** 863-869.

Cenis, J. (1992) Rapid extraction of fungal DNA for PCR amplification. *Nucleic Acids Res.* **20,** 2380.

Conesa, A. and Gotz, S. (2008) Blast2GO: A comprehensive suite for functional analysis in plant genomics. *Int. J. Plant Genomics* **2008**, Article ID 619832.

Crespo-Sempere, A., López-Pérez, M., Martínez-Culebras, P.V. and González-Candelas, L. (2011) Development of a green fluorescent tagged strain of *Aspergillus carbonarius* to monitor fungal colonization in grapes. *Int. J. Food Microbiol.* **148,** 135-140.

Crespo-Sempere, A., Selma-Lázaro, C., Martínez-Culebras, P.V. and González-Candelas, L. (2013) Characterization and disruption of the *cipC* gene in the ochratoxigenic fungus *Aspergillus carbonarius*. *Food Res. Int.* **54,** 697-705.

De Waard, M.A., Andrade, A.C., Hayashi, K., Schoonbeek, H.J., Stergiopoulos, I. and Zwiers, L.H. (2006) Impact of fungal drug transporters on fungicide sensitivity, multidrug resistance and virulence. *Pest Manage. Sci.* **62,** 195-207.

di Pietro, A., Roncero, M. and Roldán, M. (2009) From tools of survival to weapons of destruction: The role of cell wall-degrading enzymes in plant infection. In: *Plant Relationships.* The Mycota V. (Deising, H., ed.). Springer Berlin Heidelberg, pp. 181-200.

Diatchenko, L., Lau, Y.F., Campbell, A.P., Chenchik, A., Moqadam, F., Huang, B., Lukyanov, S., Lukyanov, K., Gurskaya, N., Sverdlov, E.D. and Siebert, P.D. (1996) Suppression subtractive hybridization: a method for generating differentially regulated or tissue-specific cDNA probes and libraries. *Proc. Natl. Acad. Sci. USA* **93,** 6025-6030.

Donofrio, N.M., Oh, Y., Lundy, R., Pan, H., Brown, D.E., Jeong, J.S., Coughlan, S., Mitchell, T.K. and Dean, R.A. (2006) Global gene expression during nitrogen

starvation in the rice blast fungus, *Magnaporthe grisea*. *Fungal Genet. Biol.* **43,** 605-617.

Eshel, D., Lichter, A., Dinoor, A. and Prusky, D. (2002) Characterization of *Alternaria alternata* glucanase genes expressed during infection of resistant and susceptible persimmon fruits. *Mol. Plant Pathol.* **3**, 347-358.

Eckert, J.W. (1990) Impact of fungicide resistance on citrus fruit decay control. In: *Managing Resistance to Agrochemicals.* American Chemical Society, pp. 286-302.

Eichhorn, H., Lessing, F., Winterberg, B., Schirawski, J., Kamper, J., Muller, P. and Kahmann, R. (2006) A ferroxidation/permeation iron uptake system is required for virulence in *Ustilago maydis*. *The Plant Cell* **18,** 3332-3345.

Frandsen, R.J., Andersson, J.A., Kristensen, M.B. and Giese, H. (2008) Efficient four fragment cloning for the construction of vectors for targeted gene replacement in filamentous fungi. *BMC Mol. Biol.* **9,** 70.

González-Candelas, L., Alamar, S., Sánchez-Torres, P., Zacarías, L. and Marcos, J. (2010) A transcriptomic approach highlights induction of secondary metabolism in citrus fruit in response to *Penicillium digitatum* infection. *BMC Plant Biol.* **10,** 194-211.

Haas, H., Eisendle, M. and Turgeon, B.G. (2008) Siderophores in fungal physiology and virulence. *Annu. Rev. Phytopathol.* **46,** 149-187.

Hamamoto, H., Hasegawa, K., Nakaune, R., Lee, Y.J., Makizumi, Y., Akutsu, K. and Hibi, T. (2000) Tandem repeat of a transcriptional enhancer upstream of the sterol 14 -demethylase gene (*CYP51*) in *Penicillium digitatum*. *Appl. Environ. Microbiol.* **66,** 3421-3426.

Harding, P.R. (1972) Differential sensitivity to thiabendazole by strains of *Penicillium italicum* and *P. digitatum*. *Plant Dis. Rep.* **56,** 256-260.

Isshiki, A., Akimitsu, K., Yamamoto, M. and Yamamoto, H. (2001) Endopolygalacturonase is essential for citrus black rot caused by *Alternaria citri* but not brown spot caused by *Alternaria alternata. Mol. Plant-Microbe Interact.* **14,** 749-757.

Kars, I., Krooshof, G.H., Wagemakers, L., Joosten, R., Benen, J.A.E. and van Kan, J.A.L. (2005) Necrotizing activity of five *Botrytis cinerea* endopolygalacturonases produced in *Pichia pastoris*. *Plant J.* **43,** 213-225.

Macarisin, D., Cohen, L., Eick, A., Rafael, G., Belausov, E., Wisniewski, M. and Droby, S. (2007) *Penicillium digitatum* suppresses production of hydrogen peroxide in host tissue during infection of citrus fruit. *Phytopathology* **97,** 1491-1500.

Marcet-Houben, M., Ballester, A.-R., Fuente, B., Harries, E., Marcos, J., Gonzalez-Candelas, L. and Gabaldon, T. (2012) Genome sequence of the necrotrophic fungus *Penicillium digitatum*, the main postharvest pathogen of citrus. *BMC Genomics* **13,** art. no. 646.

Marques, M.C., Alonso-Cantabrana, H., Forment, J., Arribas, R., Alamar, S., Conejero, V. and Perez-Amador, M. (2009) A new set of ESTs and cDNA clones from full-length and normalized libraries for gene discovery and functional characterization in citrus. *BMC Genomics* **10,** 428.

Mehdy, M.C. (1994) Active oxygen species in plant defense against pathogens. *Plant Physiol.* **105,** 467-472.

Moller, E.M., Bahnweg, G., Sandermann, H. and Geiger, H.H. (1992) A simple and efficient protocol for isolation of high-molecular-weight DNA from filamentous fungi, fruit bodies, and infected-plant tissues. *Nucleic Acids Res.* **20,** 6115-6116.

Naumann, T.A. and Price, N.P.J. (2012) Truncation of class IV chitinases from Arabidopsis by secreted fungal proteases. *Mol. Plant Pathol.* **13,** 1135-1139.

Palou, L., Smilanick, J.L. and Droby, S. (2008) Alternatives to conventional fungicides for the control of citrus postharvest green and blue moulds. *Stewart Postharvest Rev.* **4,** 1-16.

Poussereau, N., Creton, S., Billon-Grand, G., Rascle, C. and Fevre, M. (2001) Regulation of *acp1*, encoding a non-aspartyl acid protease expressed during pathogenesis of *Sclerotinia sclerotiorum*. *Microbiology* **147,** 717-726.

Prins, T.W., Wagemakers, L., Schouten, A. and van Kan, J.A.L. (2000) Cloning and characterization of a glutathione S-transferase homologue from the plant pathogenic fungus *Botrytis cinerea*. *Mol. Plant Pathol.* **1,** 169-178.

Rolke, Y., Liu, S., Quidde, T., Williamson, B., Schouten, A., Weltring, K.M., Siewers, V., Tenberge, K.B., Tudzynski, B. and Tudzynski, P. (2004) Functional analysis H_20_2-generating system in *Botrytis cinerea*: the major Cu-Zn superoxide dismutase (BCSOD1) contributes to virulence on French bean, whereas a glucose oxidase (BCGOD1) is dispensable. *Mol. Plant Pathol.* **5,** 17-27.

Sánchez-Torres, P. and González-Candelas, L. (2003) Isolation and characterization of genes differentially expressed during the interaction between apple fruit and *Penicillium expansum*. *Mol. Plant Pathol.* **4,** 447-457.

Schouten, A., Tenberge, K.B., Vermeer, J., Stewart, J., Wagemakers, L., Williamson, B. and Van Kan, J.A.L. (2002) Functional analysis of an extracellular catalase of *Botrytis cinerea*. *Mol. Plant Pathol.* **3,** 227-238.

Seong, K., Hou, Z., Tracy, M., Kistler, H.C. and Xu, J.R. (2005) Random insertional mutagenesis identifies genes associated with virulence in the wheat scab fungus *Fusarium graminearum*. *Phytopathology* **95,** 744-750.

Stergiopoulos, I., Zwiers, L.-H. and De Waard, M. (2002) Secretion of natural and synthetic toxic compounds from filamentous fungi by membrane transporters of the ATP-binding cassette and major facilitator superfamily. *Europ. J. Plant Pathol.* **108,** 719-734.

Sun, X., Ruan, R., Lin, L., Zhu, C., Zhang, T., Wang, M., Li, H. and Yu, D. (2013) Genomewide investigation into DNA elements and ABC transporters involved in imazalil resistance in *Penicillium digitatum*. *FEMS Microbiol. Lett.* **348,** 11-18.

ten Have, A., Mulder, W., Visser, J. and Van Kan, J.A.L. (1998) The endopolygalacturonase gene *Bcpg1* is required for full virulence of *Botrytis cinerea*. *Mol. Plant-Microbe Interact.* **11,** 1009-1016.

ten Have, A., Dekkers, E., Kay, J., Phylip, L.H. and van Kan, J.A.L. (2004) An aspartic proteinase gene family in the filamentous fungus *Botrytis cinerea* contains members with novel features. *Microbiology* **150,** 2475-2489.

ten Have, A., Espino, J.J., Dekkers, E., Van Sluyter, S.C., Brito, N., Kay, J., González, C. and van Kan, J.A.L. (2010) The *Botrytis cinerea* aspartic proteinase family. *Fungal Genet. Biol.* **47,** 53-65.

Veluchamy, S., Williams, B., Kim, K. and Dickman, M.B. (2012) The CuZn superoxide dismutase from *Sclerotinia sclerotiorum* is involved with oxidative

stress tolerance, virulence, and oxalate production. *Physiol. Mol. Plant Pathol.* **78,** 14-23.

Wang, J.Y., Sun, X.P., Lin, L.Y., Zhang, T.Y., Ma, Z.H. and Li, H.Y. (2012) PdMfs1, a major facilitator superfamily transporter from Penicillium digitatum, is partially involved in the imazalil-resistance and pathogenicity. *Afr. J. Microbiol. Res.* **6,** 95-105.

Wild, B.L., Rippon, L.E. and Seberry, J.A. (1975) Comparison of thiabendazole and benomyl as post-harvest fungicides for wastage control in long term lemon storage. *Aus. J. Exp. Agric.* **15,** 108-111.

Xu, L. and Chen, W. (2012) Random T-DNA mutagenesis identifies a Cu/Zn superoxide dismutase gene as a virulence factor of *Sclerotinia sclerotiorum*. *Mol. Plant-Microbe Interact.* **26,** 431-441.

Xu, Q., Chen, L.-L., Ruan, X., Chen, D., Zhu, A., Chen, C., Bertrand, D., Jiao, W.-B., Hao, B.-H., Lyon, M.P., Chen, J., Gao, S., Xing, F., Lan, H., Chang, J.-W., Ge, X., Lei, Y., Hu, Q., Miao, Y., Wang, L., Xiao, S., Biswas, M.K., Zeng, W., Guo, F., Cao, H., Yang, X., Xu, X.-W., Cheng, Y.-J., Xu, J., Liu, J.-H., Luo, O.J., Tang, Z., Guo, W.-W., Kuang, H., Zhang, H.-Y., Roose, M.L., Nagarajan, N., Deng, X.-X. and Ruan, Y. (2013) The draft genome of sweet orange (*Citrus sinensis*). *Nat. Genet.* **45,** 59-66.

Yan, X., Ma, W.-B., Li, Y., Wang, H., Que, Y.-W., Ma, Z.-H., Talbot, N.J. and Wang, Z.-Y. (2011) A sterol 14α-demethylase is required for conidiation, virulence and for mediating sensitivity to sterol demethylation inhibitors by the rice blast fungus *Magnaporthe oryzae*. *Fungal Genet. Biol.* **48,** 144-153.

Yakoby, N., Beno, M.D., Keen, N.T., Dinoor, A., Pines, O. and Prusky, D. (2001) *Colletotrichum gloeosporioides pelB* is an important virulence factor in avocado fruit-fungus interaction. *Mol. Plant-Microbe Interact.* **14,** 988-995.

Zhang, T., Sun, X., Xu, Q., González Candelas, L. and Li, H. (2013a) The pH signaling transcription factor PacC is required for full virulence in *Penicillium digitatum*. *Appl. Microbiol. Biotechnol.* **97,** 9087-9098.

Zhang, T., Sun, X., Xu, Q., Zhu, C., Li, Q. and Li, H. (2013b) PdSNF1, a sucrose non-fermenting protein kinase gene, is required for *Penicillium digitatum* conidiation and virulence. *Appl. Microbiol. Biotechnol.* **97,** 5433-5445.

Zhang, T., Xu, Q., Sun, X. and Li, H. (2013c) The calcineurin-responsive transcription factor Crz1 is required for conidation, full virulence and DMI resistance in *Penicillium digitatum*. *Microbiol. Res.* **168,** 211-222.

Zhao, Z., Liu, H., Wang, C. and Xu, J.-R. (2013) Comparative analysis of fungal genomes reveals different plant cell wall degrading capacity in fungi. *BMC Genomics* **14,** 274.

SUPPORTING INFORMATION

Additional Supporting Information may be found in the online version of this article:

Table S1. Annotation and relative expression in infected oranges at 3 dpi with respect to *in vitro* growth conditions of unigenes isolated from the subtracted cDNA library.

Table S2. Determination of the number of T-DNA copies integrated in the genome of *P. digitatum* transformants. Gene copy number (GC) quantification was conducted by qPCR according to the formula GC = E_{target}^($Cp_{control}$-Cp_{sample})/E_{ref}^($Cp_{control}$-Cp_{sample}). The genes *ndo1* and *pnl1* were used as the target genes for ndo1 and pnl1 transformants, respectively. The beta-tubulin gene was used as a reference and the wild type *P. digitatum* Pd1 strain was used as control. All reactions were conducted in duplicate.

Fig. S1. Estimation of the amount of *P. digitatum* RNA in infected orange tissue. Mixtures containing different proportions of RNA from *P. digitatum* (Pd) and *C. sinensis* (Cs) were separated in an agarose gel together with three replicate RNA samples from *P. digitatum*-infected oranges at 3 days post-inoculation (I3). Quantification of the fungal mitochondrial large-subunit rRNA allowed to estimate a 9:1 ratio of fungal to fruit RNA in *P. digitatum*-infected oranges at 3 days post-inoculation.

Table 1. Summary of the subtracted cDNA library PDS.

Total valid sequences	371
Sequences in contigs	269
Total number of contigs	59
Singleton sequences	102
Total number of unigenes	161
Redundancy* (%)	56.6

*Redundancy = (1-(unigenes/ESTs)) x 100

Table 2. Identification of *P. digitatum* and *C. sinensis*-responsive genes isolated from the SSH library in infected orange fruits containing three or more ESTs.

Unigen	Protein	GenBank Accesion no.	No ESTs	Description	Origin	Induction value
SSH-01	PDIP_82060	EKV05607.1	53	aspartic endopeptidase pep1	*P. digitatum*	3.51±1.47
SSH-02	PDIP_64460	EKV09364.1	16	extracellular endo-polygalacturonase 1	*P. digitatum*	2.88±1.29
SSH-03	PDIP_65210	EKV09439.1	13	extracellular endoglucanase/cellulase	*P. digitatum*	1.75±0.87
SSH-04	PDIP_06020	EKV21461.1	13	aspergillopepsin	*P. digitatum*	3.88±1.19
SSH-05	PDIP_12220	EKV20850.1	12	tripeptidyl peptidase I	*P. digitatum*	3.12±1.13
SSH-06	PDIP_45260	EKV14128.1	10	CipC1 protein, concanamycin induced	*P. digitatum*	3.81±1.35
SSH-07	PDIP_03330	EKV21742.1	9	hypothetical protein	*P. digitatum*	1.15±0.39
SSH-08	PDIP_71590	EKV07879.1	7	carboxypeptidase 5	*P. digitatum*	1.96±0.58
SSH-09	mitochondrion	CM001644.1	7	*Penicillium digitatum* Pd1	*P. digitatum*	0.80±0.22
SSH-10	PDIP_47870	EKV13428.1	6	GAPDH precursor	*P. digitatum*	1.86±1.03
SSH-11	PDIP_77270	EKV06691.1	6	extracellular guanyl-specific	*P. digitatum*	2.67±1.03
SSH-12	Cs2g10140.1		6	reticuline oxidase	*C. sinensis*	0.96±0.27
SSH-13	PDIP_33560	EKV16989.1	5	hypothetical protein	*P. digitatum*	1.32±0.12
SSH-14	PDIP_45660	EKV13970.1	4	sorbitol/xylulose reductase	*P. digitatum*	1.39±0.21
SSH-15	PDIP_08080	EKV21276.1	3	pectin lyase 1	*P. digitatum*	2.07±0.11
SSH-16	PDIP_49840	EKV13126.1	3	translation initiation inhibitor	*P. digitatum*	2.04±0.11
SSH-17	Cs2g28680.1		3	pathogen-inducible alpha-dioxygenase	*C. sinensis*	2.60±1.14
SSH-18	PDIP_48830	EKV13195.1	3	nucleoside diphosphate kinase	*P. digitatum*	1.79±0.47
SSH-19	PDIP_49850	EKV13127.1	3	gibberellin 3-beta hydroxylase	*P. digitatum*	0.99±0.50
SSH-20	Cs3g01585.1		3	DNA binding protein	*C. sinensis*	1.27±0.09
SSH-21	PDIP_06490	EKV21440.1	3	hypothetical protein	*P. digitatum*	1.32±0.29
SSH-22	PDIP_10140	EKV21060.1	3	naphthalene 1,2-dioxygenase subunit	*P. digitatum*	1.11±0.21
SSH-23	PDIP_41510	EKV15092.1	3	60S ribosomal protein	*P. digitatum*	1.24±0.33
SSH-24	PDIP_57790	EKV11104.1	3	pectin lyase	*P. digitatum*	2.46±0.00
SSH-25	PDIP_64200	EKV09493.1	3	branched-chain amino acid	*P. digitatum*	1.22±0.15
SSH-26	PDIP_67670	EKV08475.1	3	serine peptidase, family S28	*P. digitatum*	1.93±1.70

Table 3. Genes with a 2-fold or higher induction level at 3 days post infection in orange fruits inoculated with *P. digitatum* with respect to *in vitro* growth conditions.

Unigen	Protein	GenBank Accesion no.	No ESTs	Description	Origin	Induction value
SSH-38	PDIP_76190	EKV06798.1	2	extracellular thaumatin domain protein	*P. digitatum*	4.16±0.59
PDS15G06	chr. 7		1	between Cs7g25660 and Cs7g25670	*C. sinensis*	4.07
SSH-04	PDIP_06020	EKV21461.1	13	aspergillopepsin	*P. digitatum*	3.88±1.19
SSH-06	PDIP_45260	EKV14128.1	10	CipC1 protein, concanamycin induced protein	*P. digitatum*	3.81±1.35
SSH-46	PDIP_12700	EKV20803.1	2	hypothetical protein	*P. digitatum*	3.68
SSH-01	PDIP_82060	EKV05607.1	53	aspartic endopeptidase pep1	*P. digitatum*	3.51±1.47
PDS01H10	PDIP_61480	EKV10010.1	1	hypothetical protein	*P. digitatum*	3.44
SSH-34	PDIP_40860	EKV15256.1	2	FAD binding domain protein	*P. digitatum*	3.43±0.40
SSH-05	PDIP_12220	EKV20850.1	12	protease S8 tripeptidyl peptidase I	*P. digitatum*	3.12±1.13
SSH-02	PDIP_64460	EKV09364.1	16	extracellular endo-polygalacturonase 1	*P. digitatum*	2.88±1.29
SSH-11	PDIP_77270	EKV06691.1	6	extracellular guanyl-specific ribonuclease	*P. digitatum*	2.67±1.03
SSH-17	Cs2g28680.1		3	pathogen-inducible alpha-dioxygenase	*C. sinensis*	2.60±1.14
PDS09G03	PDIP_27790	EKV18231.1	1	aflatoxin b1 aldehyde reductase-like protein	*P. digitatum*	2.53
SSH-24	PDIP_57790	EKV11104.1	3	pectin lyase	*P. digitatum*	2.46
PDS08F04	PDIP_42980	EKV14602.1	1	NADP(+)-dependent glycerol dehydrogenase	*P. digitatum*	2.42
SSH-32	PDIP_23200	EKV19512.1	2	hypothetical protein	*P. digitatum*	2.23±0.14
SSH-30	PDIP_07830	EKV21285.1	2	sarcosine oxidase	*P. digitatum*	2.22±0.29
PDS08G09	PDIP_71990	EKV07821.1	1	ribosomal protein L34 protein	*P. digitatum*	2.21
PDS02H01	PDIP_15790	EKV20495.1	1	60S ribosomal protein L13	*P. digitatum*	2.20
SSH-15	PDIP_08080	EKV21276.1	3	pectin lyase 1	*P. digitatum*	2.07±0.11
SSH-50	PDIP_70570	EKV08094.1	2	pyruvate kinase	*P. digitatum*	2.07±1.69
SSH-16	PDIP_49840	EKV13126.1	3	translation initiation inhibitor	*P. digitatum*	2.04±0.11
PDS09F01	PDIP_55120	EKV11691.1	1	phytase	*P. digitatum*	2.03

Table 4. Oligonucleotides used in the present work

Name	Sequence
betatubPDIG1	CGATGGCGATGGACAGTAAGTTT
betatubPDIG2	TTGGTTCGTGGTCGTTGTACTCA
FOR17	GTAAAACGACGGCCAGT
HMBF1	CTGTCGAGAAGTTTCTGATCG
HMBR1	CTGATAGAGTTGGTCAAGACC
N2R	AGCGTGGTCGTCGCGGCCCGAGGT
PL1A	TAGTGCTGACGACCAATG
PL1S	CGAGGAGCTGGTCTCTTA
PL5A	TCAATTAATACGGGGCTAGA
PL6S	CAAGATAGAACACCCACAACT
PLA3	GGACTTAAUTCGGGGCAATTGCTTCGCTACACCA
PLA4	GGGTTTAAUGCCGACCTAACTTTAGGGGCACCCAGTT
PLO1	GGTCTTAAUTACACTATCCCCAAGCCCCGGCGTA
PLO2	GGCATTAAUGGGCTTTGTTACCGCCATTCGATCTCC
PLPrA	CCATAGGGAGTAGTGTGACGTGTTC
PLPrS	CACAACATAGGGCGACCTAATCC
RP5A	TTAACAACCACACCAGTATCC
RP6S	GAGATTGAGGATTCGCATAG
RP7S	TGCATCATGGTACACTTCAC
RP8A	CGTGGATTCGCAGTGGTGTT
RPA3	GGACTTAAUGCGAAGCCGAAGGTGACATGCAACG
RPA4	GGGTTTAAUTCCCGAGGCATATTTTGCAACTGTGGA
RPO1	GGTCTTAAUTACCCGGGGATCCCACGTACAACGA
RPO2	GGCATTAAUGCCAGGCGGGTTGAACTTCCGAAAA
RPPrA	CCGAGTAGAGGTTGGGTTTGACA
RPPrS	CCACCACAGCACTACAATCCGTACT
SP6	GATTTAGGTGACACTATAGAATAC

A

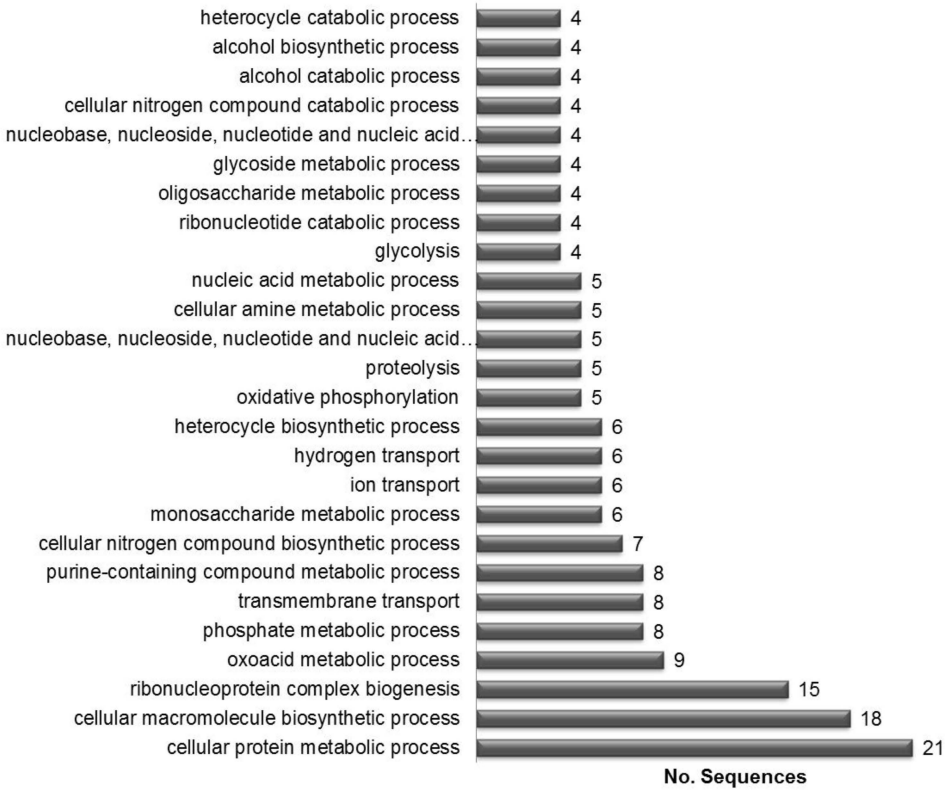
heterocycle catabolic process 4
alcohol biosynthetic process 4
alcohol catabolic process 4
cellular nitrogen compound catabolic process 4
nucleobase, nucleoside, nucleotide and nucleic acid… 4
glycoside metabolic process 4
oligosaccharide metabolic process 4
ribonucleotide catabolic process 4
glycolysis 4
nucleic acid metabolic process 5
cellular amine metabolic process 5
nucleobase, nucleoside, nucleotide and nucleic acid… 5
proteolysis 5
oxidative phosphorylation 5
heterocycle biosynthetic process 6
hydrogen transport 6
ion transport 6
monosaccharide metabolic process 6
cellular nitrogen compound biosynthetic process 7
purine-containing compound metabolic process 8
transmembrane transport 8
phosphate metabolic process 8
oxoacid metabolic process 9
ribonucleoprotein complex biogenesis 15
cellular macromolecule biosynthetic process 18
cellular protein metabolic process 21
No. Sequences

B

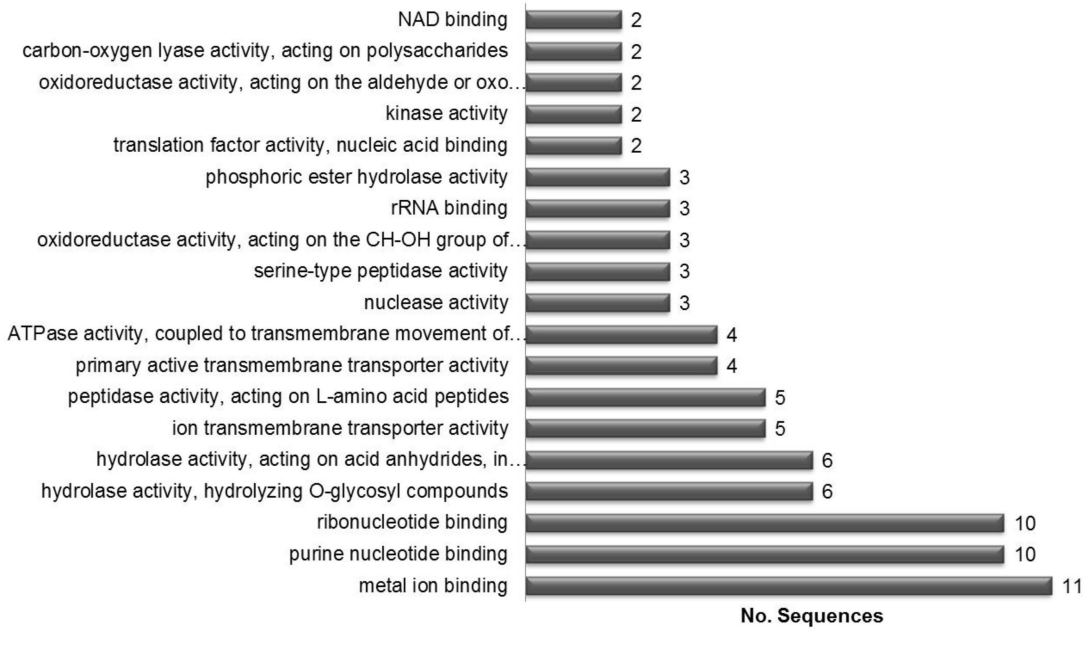
NAD binding 2
carbon-oxygen lyase activity, acting on polysaccharides 2
oxidoreductase activity, acting on the aldehyde or oxo… 2
kinase activity 2
translation factor activity, nucleic acid binding 2
phosphoric ester hydrolase activity 3
rRNA binding 3
oxidoreductase activity, acting on the CH-OH group of… 3
serine-type peptidase activity 3
nuclease activity 3
ATPase activity, coupled to transmembrane movement of… 4
primary active transmembrane transporter activity 4
peptidase activity, acting on L-amino acid peptides 5
ion transmembrane transporter activity 5
hydrolase activity, acting on acid anhydrides, in… 6
hydrolase activity, hydrolyzing O-glycosyl compounds 6
ribonucleotide binding 10
purine nucleotide binding 10
metal ion binding 11
No. Sequences

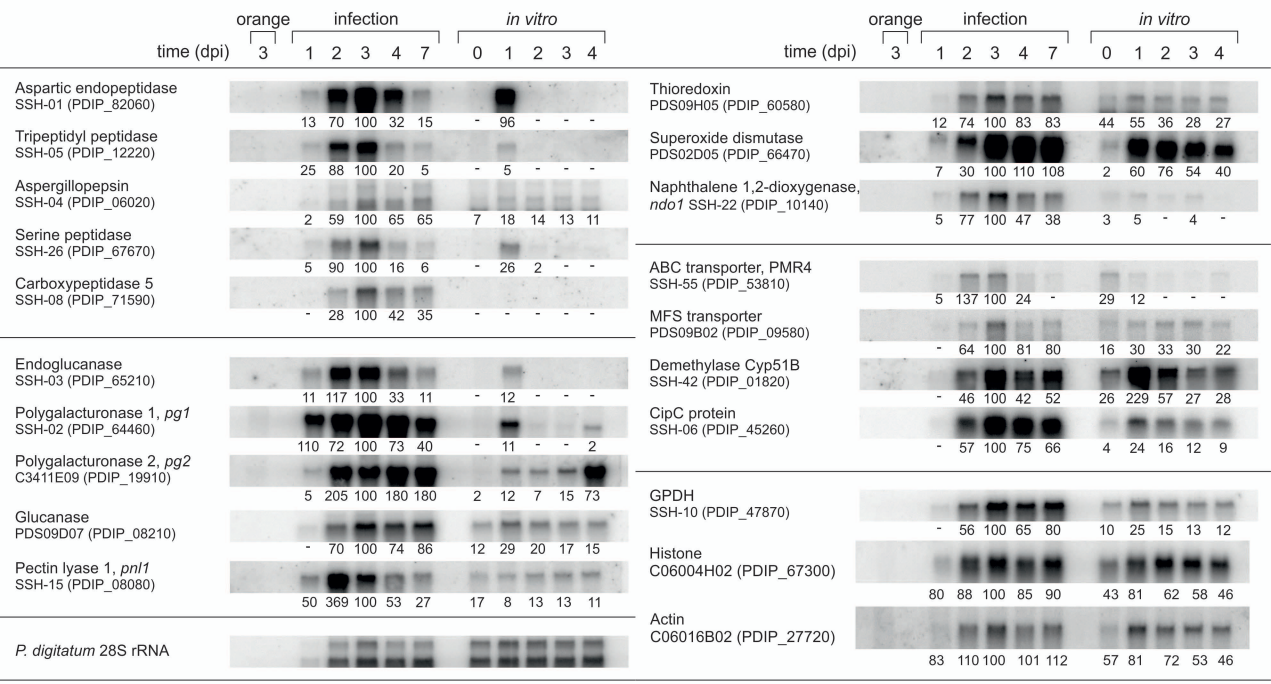
orange
infection
in vitro
time (dpi)
3
1 2 3 4 7
0 1 2 3 4
Aspartic endopeptidase
SSH-01 (PDIP_82060)
13 70 100 32 15 - 96 - - -
Tripeptidyl peptidase
SSH-05 (PDIP_12220)
25 88 100 20 5 - 5 - - -
Aspergillopepsin
SSH-04 (PDIP_06020)
2 59 100 65 65 7 18 14 13 11
Serine peptidase
SSH-26 (PDIP_67670)
5 90 100 16 6 - 26 2 - -
Carboxypeptidase 5
SSH-08 (PDIP_71590)
- 28 100 42 35 - - - - -
Endoglucanase
SSH-03 (PDIP_65210)
11 117 100 33 11 - 12 - - -
Polygalacturonase 1, pg1
SSH-02 (PDIP_64460)
110 72 100 73 40 - 11 - - 2
Polygalacturonase 2, pg2
C3411E09 (PDIP_19910)
5 205 100 180 180 2 12 7 15 73
Glucanase
PDS09D07 (PDIP_08210)
- 70 100 74 86 12 29 20 17 15
Pectin lyase 1, pnl1
SSH-15 (PDIP_08080)
50 369 100 53 27 17 8 13 13 11
P. digitatum 28S rRNA
orange
infection
in vitro
time (dpi)
3
1 2 3 4 7
0 1 2 3 4
Thioredoxin
PDS09H05 (PDIP_60580)
12 74 100 83 83 44 55 36 28 27
Superoxide dismutase
PDS02D05 (PDIP_66470)
7 30 100 110 108 2 60 76 54 40
Naphthalene 1,2-dioxygenase,
ndo1 SSH-22 (PDIP_10140)
5 77 100 47 38 3 5 - 4 -
ABC transporter, PMR4
SSH-55 (PDIP_53810)
5 137 100 24 - 29 12 - - -
MFS transporter
PDS09B02 (PDIP_09580)
- 64 100 81 80 16 30 33 30 22
Demethylase Cyp51B
SSH-42 (PDIP_01820)
- 46 100 42 52 26 229 57 27 28
CipC protein
SSH-06 (PDIP_45260)
- 57 100 75 66 4 24 16 12 9
GPDH
SSH-10 (PDIP_47870)
- 56 100 65 80 10 25 15 13 12
Histone
C06004H02 (PDIP_67300)
80 88 100 85 90 43 81 62 58 46
Actin
C06016B02 (PDIP_27720)
83 110 100 101 112 57 81 72 53 46

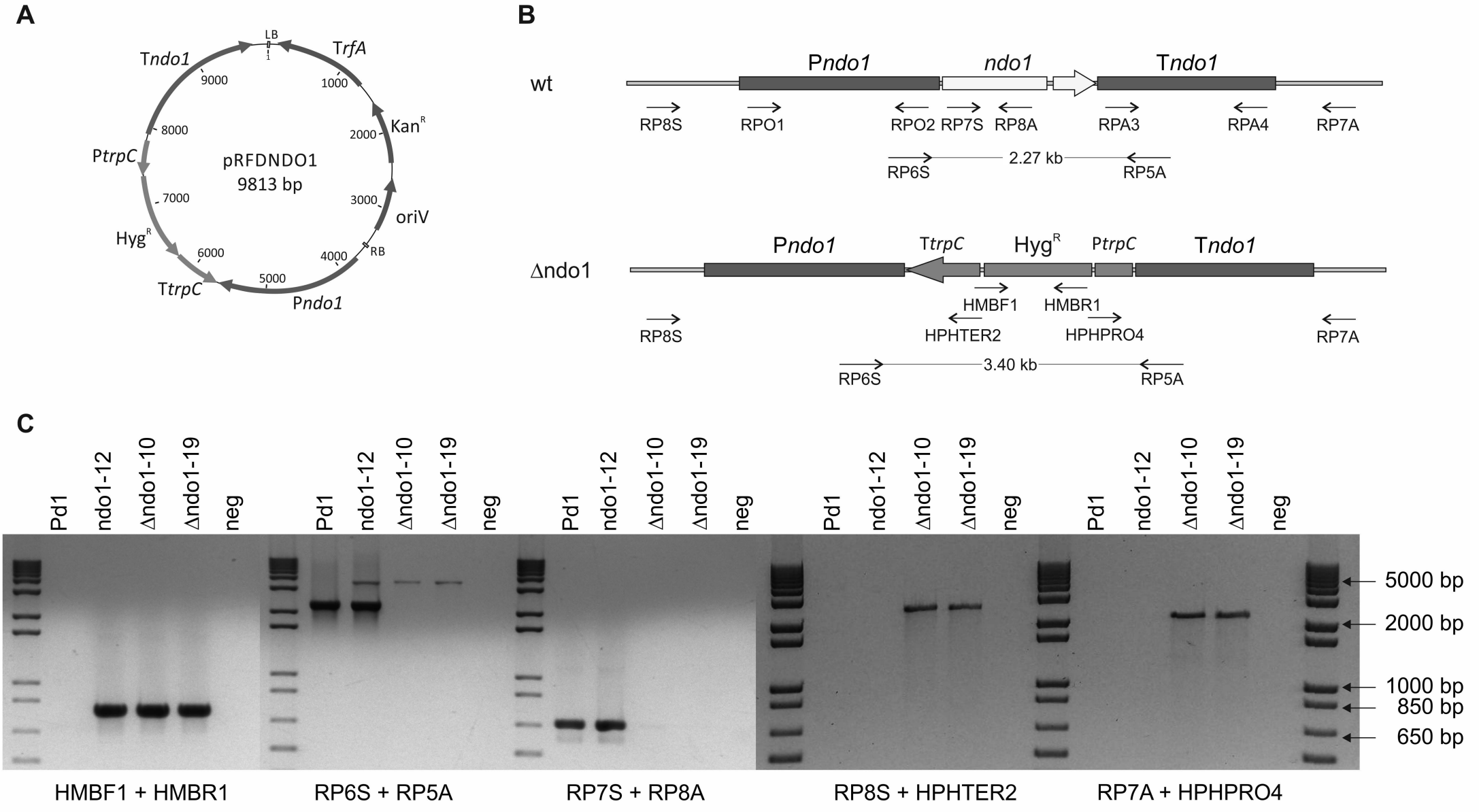
A
LB
TrfA
Kan^R
oriV
RB
PtrpC
Hyg^R
TtrpC
Pndo1
Tndo1
pRFDNDO1
9813 bp
1000
2000
3000
4000
5000
6000
7000
8000
9000
B
wt
Pndo1
ndo1
Tndo1
RP8S
RPO1
RPO2
RP7S
RP8A
RPA3
RPA4
RP7A
RP6S
2.27 kb
RP5A
Δndo1
TtrpC
Hyg^R
PtrpC
HMBF1
HMBR1
HPHTER2
HPHPRO4
3.40 kb
C
Pd1
ndo1-12
Δndo1-10
Δndo1-19
neg
5000 bp
2000 bp
1000 bp
850 bp
650 bp
HMBF1 + HMBR1
RP6S + RP5A
RP7S + RP8A
RP8S + HPHTER2
RP7A + HPHPRO4

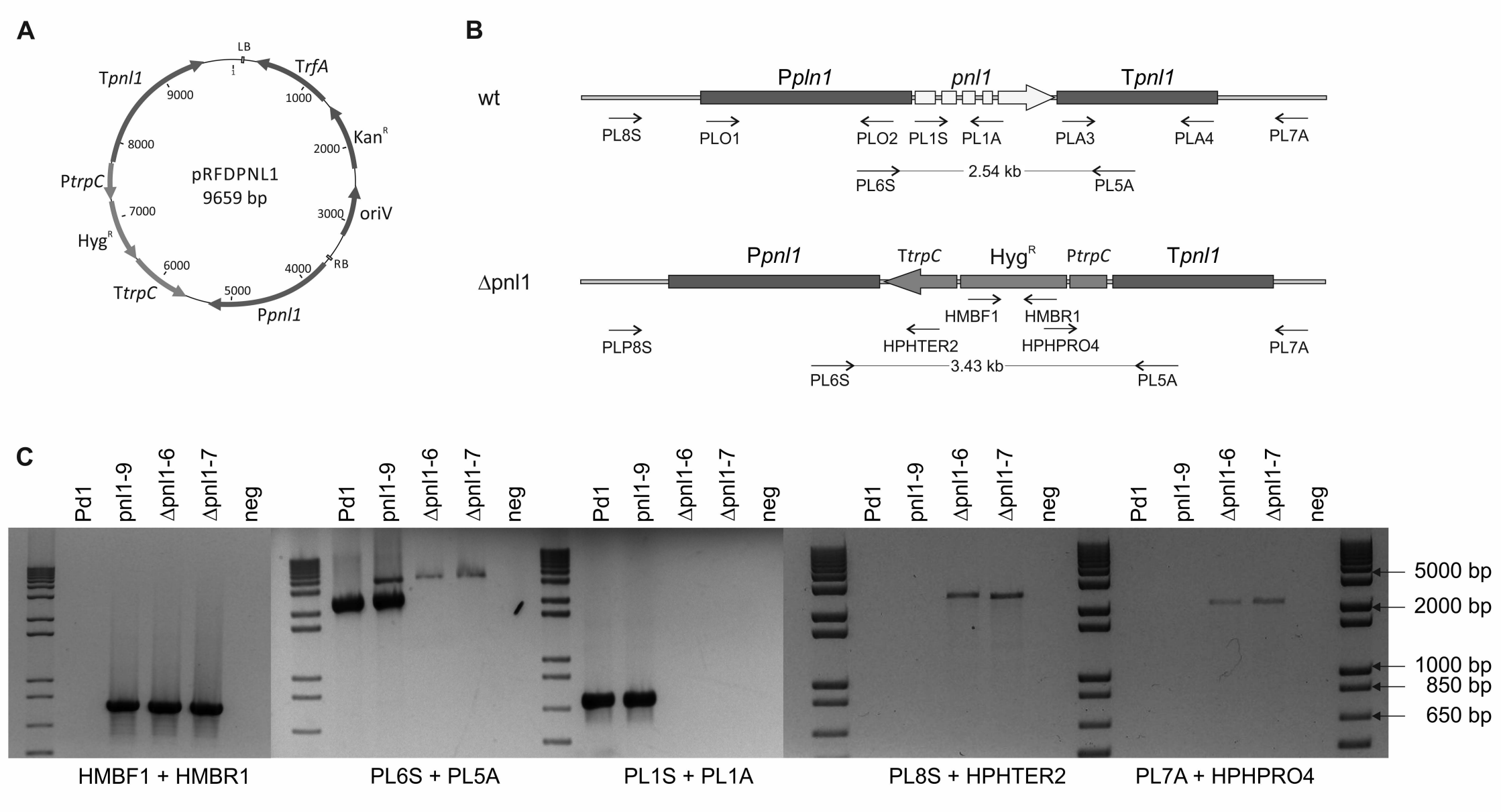
A
LB
TrfA
Kan^R
oriV
RB
Ppnl1
TtrpC
Hyg^R
PtrpC
Tpnl1
pRFDPNL1
9659 bp
1
1000
2000
3000
4000
5000
6000
7000
8000
9000
B
wt
Ppln1
pnl1
Tpnl1
PL8S
PLO1
PLO2
PL1S
PL1A
PLA3
PLA4
PL7A
PL6S
2.54 kb
PL5A
Δpnl1
Ppnl1
TtrpC
Hyg^R
PtrpC
Tpnl1
HMBF1
HMBR1
PLP8S
HPHTER2
HPHPRO4
PL7A
PL6S
3.43 kb
PL5A
C
Pd1
pnl1-9
Δpnl1-6
Δpnl1-7
neg
5000 bp
2000 bp
1000 bp
850 bp
650 bp
HMBF1 + HMBR1
PL6S + PL5A
PL1S + PL1A
PL8S + HPHTER2
PL7A + HPHPRO4

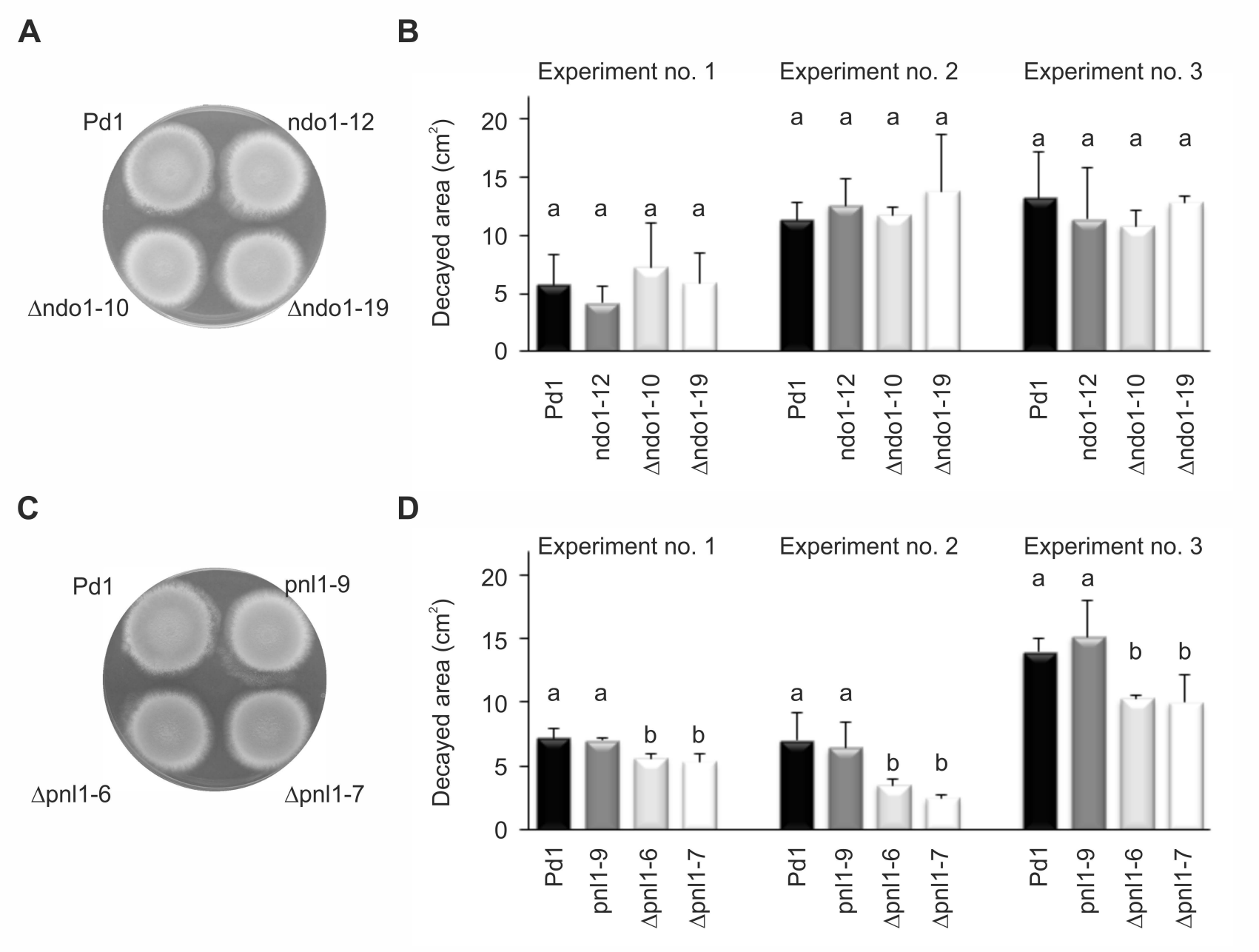
A
Pd1
ndo1-12
Δndo1-10
Δndo1-19
B
Experiment no. 1
Experiment no. 2
Experiment no. 3
Decayed area (cm2)
0
5
10
15
20
a
Pd1
ndo1-12
Δndo1-10
Δndo1-19
C
Pd1
pnl1-9
Δpnl1-6
Δpnl1-7
D
Experiment no. 1
Experiment no. 2
Experiment no. 3
Decayed area (cm2)
a
b
Pd1
pnl1-9
Δpnl1-6
Δpnl1-7